Amplified mid-latitude planetary waves favour particular regional weather extremes

James A. Screen[1] & Ian Simmonds[2]

[1]*College of Engineering, Mathematics and Physical Sciences, University of Exeter, Exeter EX4 4QF, UK.*

[2]*School of Earth Sciences, The University of Melbourne, Melbourne, Victoria 3010, Australia.*

There has been an ostensibly large number of extreme weather events in the northern hemisphere mid-latitudes during the last decade[1]. An open question that is critically important for scientists and policy makers is whether any such increase in weather extremes is natural or anthropogenic in origin[2-14]. One mechanism proposed to explain the increased frequency of extreme weather events is the amplification of mid-latitude atmospheric planetary waves[15-17]. Disproportionately large warming in the northern polar regions compared to mid-latitudes – and associated weakening of the north-south temperature gradient - may favour larger amplitude planetary waves[15,17], although observational evidence for this remains inconclusive[18-20]. A better understanding of the role of planetary waves in causing mid-latitude weather extremes is essential for assessing the potential environmental and socio-economic impacts of future planetary wave changes. Here we show that months of extreme weather over mid-latitudes are commonly accompanied by

significantly amplified quasi-stationary mid-tropospheric planetary waves, with zonal wave numbers of 3-8. Conversely, months of near-average weather over mid-latitudes are often accompanied by significantly attenuated wave numbers 3-8. Depending on geographical region, certain types of extreme weather (e.g., hot, cold, wet, dry) are more strongly related to wave amplitude changes than others. The findings suggest that amplification of quasi-stationary wave numbers 3-8 preferentially increases the probabilities of heat waves in western North America and central Asia, cold outbreaks in eastern North America, droughts in central North America, Europe and central Asia, and wet spells in western Asia.

A series of weather extremes have hit the Northern Hemisphere mid-latitudes in the recent years[1], such as the European heat wave in summer 2003[8], cold and snowy winters in 2009/10, 2010/11 and 2013/14 in northeast United States[16], the Russian heat wave in summer 2010[2-5], Texas drought of 2011[6], and the summer 2012 and winter 2013/14 floods in United Kingdom[7]; all have had significant socio-economic impacts. There is increasing scientific evidence[1-14] and a growing public perception[21] that extreme weather events are occurring more frequently. However, the mechanisms that drive weather extremes and through which climate change may influence climate variability are poorly understood. A potential cause of increased weather extremes is the amplification of atmospheric planetary waves[15-17]. Empirical[15,16] , dynamical[17] and modelling[16,22] evidence suggest a weakening north-south temperature gradient – a key characteristic of anthropogenic climate change[23,24] – causes larger amplitude planetary waves, and it is hypothesised that high-amplitude planetary waves favour the occurrence of extreme weather. It is this hypothesis that we examine here.

First, it is necessary to define precisely "extreme weather" for this application. We are concerned with persistent anomalies in land surface temperature (T_L) and land precipitation (P_L), such as heat waves, cold spells, droughts and prolonged wet periods, which are evident on monthly timescales and large spatial scales (see Methods). Initially we focus on absolute (i.e., irrespective of their sign) T_L and P_L anomalies (denoted $|T_L'|$ and $|P_L'|$). This is appropriate because planetary waves tend to induce positive T_L (and perhaps P_L) anomalies at some longitudes and negative anomalies at other longitudes.

Fig. 1a,b show normalized time-series for monthly $|T_L'|$ and $|P_L'|$, respectively, area-averaged over northern mid-latitudes (35-60°N; ML). The 40 months with largest values (approx. 10% of cases) are highlighted by circles and labelled on the lower x-axis. The months of extreme T_L and P_L lie relatively evenly through the 34-year period, and there is no long-term trend. A full discussion of 34-year trends in $|T_L'|$ and $|P_L'|$ is provided in the Supplementary Discussion S1. Fig. 1c shows planetary-wave amplitude anomalies (normalized by removing the mean amplitude and dividing by the standard deviation, σ, for each wave number) for wave numbers 3-8 during months of T_L extremes (i.e., the months shown by circles in Fig. 1a). The overwhelming majority of the statistically significant amplitude anomalies are positive. The number of significant positive anomalies (32) is appreciably larger than would be expected by chance alone (12). On half of the extreme months considered there is at least one significant positive amplitude anomaly for wave numbers 3-8. The three months with significant negative amplitude anomalies also have at least one significant positive amplitude anomaly. Thus, it would appear that some wave numbers are amplified at the expense of other wave numbers. Although significantly amplified planetary-waves are common during months of T_L extremes, it is not always the same wave number(s) that is/are amplified. The greatest number of significant positive amplitude anomalies are found for wave numbers 5, 6 and 7. Positive monthly-mean amplitude anomalies imply, in physical terms, highly meridional and persistent (slow-moving) circulation regimes (see Supplementary Discussion S2).

The statistically significant planetary-wave amplitude anomalies during months of P_L extremes (i.e., the months shown by circles in Fig. 1b) are also predominantly positive (Fig. 1d). Significantly amplified waves, in at least one wave number 3-8, are identified in 40% of the months with extreme P_L. This percentage increases to 50% for the 20 months with most extreme P_L. In contrast, only one of these 20 months displays a significant negative amplitude anomaly and further, this is accompanied by positive anomalies in two other wave numbers. As for T_L, this suggests a link between extreme P_L and significantly amplified planetary waves. However, clearly not all months with T_L or P_L extremes are associated with significantly amplified, or attenuated, planetary-wave amplitudes.

Fig. 2a shows the probability density function (PDF) of amplitude anomalies for each of wave numbers 3-8 in each of the 40 months of T_L extremes. Months of T_L

extremes over ML are associated with significantly amplified planetary waves, in the sense that positive amplitude anomalies occur relatively more often during months of T_L extremes than they do climatologically. The difference in mean amplitude anomalies, between extreme months and climatology, is very highly statistically significant ($p < 0.001$). The difference in amplitude variance is also highly significant ($p < 0.01$), with greater variance in months of T_L extremes than climatologically. This increase in variance is primarily due to larger frequencies at the positive tail of the distribution. This suggests that not only are T_L extremes associated with amplified waves on average, but also that there is an particularly strong association between the most highly amplified planetary waves and extreme T_L.

On the basis of daily reanalysis data, it can be seen that planetary-wave amplitude and $|T_L'|$ co-vary almost simultaneously, but with the temperature anomalies lagging the amplitude anomalies by 1-2 days (Supplementary Figure 3). This time lag implies that surface temperatures are responding to the atmospheric circulation anomalies and not the other way round. Furthermore, whilst surface temperatures respond very rapidly to circulation changes (hours to days), the timescale for the mid-tropospheric circulation (wave amplitude is defined at 500 hPa; see Methods) to respond to surface temperature anomalies is much slower (tens of days to months). Thus irrespective of the small time lag, the timescale of the response is strongly suggestive of a causal link between planetary-wave amplitude and temperature extremes (see Supplementary Discussion S3).

Fig. 2b-h show PDFs for the planetary-wave amplitude anomalies during months with T_L extremes over seven geographical regions (shown in Fig. 3). Over wNAm, cNAm and Euro, T_L extremes are associated with significantly larger mean amplitude and greater amplitude variance, consistent with the results for ML. T_L extremes over eNAm are linked to increased amplitude variance, but not significantly different mean amplitude. Over eAsia, significantly attenuated planetary-wave amplitudes accompany T_L extremes.

Analogous PDFs for months of P_L extremes are shown in Fig. 2i-p. As for T_L extremes, we find that P_L extremes over ML are associated with significantly larger mean amplitude and significantly larger variance (again, the latter is primarily due to greater frequencies at the positive tail of the PDF). Regional P_L extremes over wNAm, Euro and wAsia are also linked to significantly amplified waves.

The association between planetary-wave amplitude and mid-latitude- mean $|T_L'|$ exists over a wide range of timescales from daily to sub-seasonal. The strength of this relationship is relatively insensitive to timescale, although is it marginally strongest on 5-14 day timescales (Supplementary Discussion S5). In contrast, the amplitude-precipitation relationship weakens for timescales less than 12 days. This implies that planetary waves are more important for longer-duration precipitation extremes, such as those that contribute to drought, than they are for short-lived precipitation extremes. We speculate that precipitation variability is closely related to synoptic- or local-scale drivers on short timescales whereas longer-lived events are more closely tied to the large-scale atmospheric circulation.

If extreme weather is linked to amplified waves, is near-average weather accompanied by attenuated planetary waves? Months of near-average (see Methods for definition) T_L over ML and wNAm are associated with, on average, significantly attenuated planetary-wave amplitudes, whereas months of near-average T_L over eAsia are accompanied by significantly amplified waves (Fig. 3). All these relationships are opposite to those found for months with extreme T_L. In Euro and wAsia, amplitude variance is significantly lower in months of extreme T_L than climatologically. From the PDFs, it can be seen that this primarily reflects fewer cases of large positive amplitude anomalies during the months of near-average T_L than climatologically. Whilst months with T_L extremes are often accompanied by highly amplified waves, these rarely accompany months with near-average T_L. Turning to precipitation, none of the geographical regions show a significant difference in mean amplitude anomaly between months of near-average P_L and climatology (Fig. 3i-p). However, amplitude variance is significantly lower over ML and wNAm, as a consequence of fewer (in percentage terms) large positive amplitude anomalies during months of near-average P_L than in all months taken together.

It is reasonable to expect that any particular planetary wave will induce positive T_L (and perhaps P_L) anomalies at some longitudes and negative anomalies at other longitudes. If wave phase was highly variable in time (i.e., the waves were "free"), amplified waves might favour extremes of both sign (hot or cold, wet or dry) at any specific longitude. However in reality, the waves have preferred phases (i.e., they are quasi-stationary), related to orography and climatological-mean thermal gradients[15,25]. This is especially the case for the smaller wave numbers. Further, at any particular location, T_L and P_L may be more sensitive to amplitude anomalies of one sign than the other, or to some wave numbers and phases than others. Therefore, amplified waves may in fact favour one type of extreme weather more than another, in any specific location. Table 1 compares the mean amplitude and variance in regionally hot, cold, wet and dry months to climatological mean amplitude and variance (the full PDFs are shown in Supplementary Discussion S5). Consistent with the rationale above, it appears that in most regions there are stronger links between planetary-wave amplitude and weather extremes of one sign than extremes of the other. Significantly amplified waves are found during hot extremes over wNAm and cAsia, cold extremes over eNAm, dry extremes over Euro and cAsia, and wet extremes over wAsia. In each case, extremes of opposite sign in the same region are not accompanied by significantly amplified, or attenuated, planetary waves. Precipitation extremes over cNAm are an interesting case: amplified waves tend to accompany dry extremes whereas attenuated waves preferentially occur during wet extremes.

These findings reinforce suggestions that amplified planetary waves favour extreme weather in mid-latitudes[15-17,26]. However, previous studies have not determined which types of extreme weather are caused by amplified waves, or where these extremes are likely to occur. Clearly these details are critically important for decision makers in assessing the risk of, and planning for the impacts of, extreme weather events in the future. If quasi-stationary wave numbers 3-8 are amplified in response to anthropogenic climate change, as has been proposed[15,17], our results suggest that this would preferentially increase the probabilities of heat waves in western North America and central Asia, cold waves in eastern North America, droughts in central North America, Europe and central Asia, and wet extremes in western Asia. However, robust observational evidence for long-term trends in planetary-wave amplitude is lacking[18-20] and further work is required to understand better the physical mechanisms through which human-induced climate change may impact upon mid-latitude planetary waves.

Methods

Observations. Monthly-mean T_L and P_L from January 1979 to December 2012 were taken from the CRUTEM4 and GPCP v2.2 data sets, respectively. CRUTEM4 data[27] are derived from in situ observations at meteorological stations. GPCP data[28] are derived from a combination of in situ measurements and satellite estimates. For this study, GPCP data were re-gridded to the CRUTEM4 grid (5° by 5° longitude-latitude). The global-mean T_L and P_L have been subtracted from the grid-box values. This procedure removed global-mean variability and trends, but retained regional signatures such as those associated with planetary wave changes.

Extremes. We derived T_L and P_L anomalies (denoted T_L' and P_L') by removing the relevant climatological monthly mean at each grid-box. Absolute values (i.e., the modulus) of T_L' and P_L' (denoted $|T_L'|$ and $|P_L'|$) are used to describe the magnitude of the anomalies irrespective of their sign. This is appropriate because planetary waves tend to induce positive T_L (and perhaps P_L) anomalies at some longitudes and negative anomalies at other longitudes. Grid-point anomalies were area-averaged over eight geographical regions: mid-latitudes (ML; 35-60°N, 180°E-180°W), western North America (wNAm; 35-60°N, 115-150°W), central North America (cNAm; 35-60°N, 80-115°W), eastern North America (eNAm; 35-60°N, 45-80°W), Europe (Euro; 35-60°N, 25°E-15°W), western Asia (wAsia; 35-60°N, 25-65°E), central Asia (cAsia; 35-60°N, 65-105°E) and eastern Asia (eAsia; 35-60°N, 105-145°E). These regions (shown in Fig. 3) were chosen *a priori* based on conventional (sub-) continental boundaries and are approximately equal in area and together they cover all the mid-latitude landmasses. The area-averaged monthly time-series were normalised by removing the climatological mean and dividing by the standard deviation for each calendar month. For each region, we then defined "extreme months" as the 40 cases (approximately 10%) with largest $|T_L'|$ or $|P_L'|$; and "near-average" months as the 40 cases with smallest $|T_L'|$ or $|P_L'|$. "Hot", "cold", "wet" and "dry" months are defined based on the 40 months with largest T_L', smallest T_L', largest P_L' and smallest P_L', respectively. The selected years are provided in Supplementary Discussion S6.

Wave amplitude. We analyse amplitudes of planetary waves in the monthly-mean mid-tropospheric mid-latitude circulation, with zonal wave numbers 3-8. Amplitudes were defined based upon Fourier analysis of 500 hPa geopotential heights (Z_{500}), meridionally averaged over mid-latitudes (35-60°N), as a function of longitude. Monthly-mean Z_{500} were taken from the ERA-Interim reanalysis[29]. This approach is consistent with the "zonal amplitude" metric used in ref. 18, except here we use monthly-mean Z_{500} averaged over latitudes 35-60°N rather than daily values at 45°N. Whilst multi-decadal trends in planetary-wave amplitude are sensitive to how amplitude is defined[18,20], month-to-month variability of amplitude is highly consistent using the two frameworks outlined in ref. 18. In this manuscript we exclusively consider amplitude variability (not trends) and thus, use only one definition of planetary-wave amplitude.

Statistics. Differences in sample means were assessed using an unequal variance t-test. This is an adaptation of the Student's t-test that accounts for the two samples having different sizes and possibly unequal variances[30]. Differences in sample variance were assessed using a Fisher f-test. We tested against the null hypothesis that the two sample means or variances are equal. The null hypothesis was rejected if the probability of equal means or variances is less than 10% ($p < 0.1$).

References

1. Coumou, D. & Rahmstorf, S. A decade of weather extremes. *Nature Clim. Change* **2**, 491-496 (2012).
2. Rahmstorf, S. & Coumou, D. Increase of extreme events in a warming world. *Proc. Natl. Acad. Sci. USA.* **108**, 17905–17909 (2011).
3. Dole, R. *et al*. Was there a basis for anticipating the 2010 Russian heat wave? *Geophys. Res. Lett.* **38**, L06702 (2011).
4. Otto, F. E. L., Massey, N., van Oldenborgh, G. J., Jones, R. G. & Allen, M. R. Reconciling two approaches to attribution of the 2010 Russian heat wave. *Geophys. Res. Lett.* **39**, L04702 (2012).

5. Trenberth, K. E. & Fasullo, J. Climate extremes and climate change: The Russian heat wave and other climate extremes of 2010. *J. Geophys. Res.* **117**, D17103 (2012).

6. Peterson, T. C., Stott, P. A. & Herring, S. Explaining extreme events of 2011 from a climate perspective. *Bull. Amer. Meteor. Soc.* **93**, 1041–1067 (2012).

7. Peterson, T. C., Hoerling, M. P., Stott, P. A. & Herring, S. C. Explaining extreme events of 2012 from a climate perspective. *Bull. Amer. Meteor. Soc.* **94**, S1-S74 (2013).

8. Stott, P. A., Stone, D. A. & Allen, M. R. Human contribution to the European heatwave of 2003. *Nature* **432**, 610–614 (2004).

9. Zwiers, F. W., Zhang, X. & Feng, Y. Anthropogenic influence on long return period daily temperature extremes at regional scales. *J. Clim.* **24**, 881–892 (2011).

10. Dai, A. Drought under global warming: a review. *WIREs Clim. Change* **2**, 45–65 (2011).

11. Pall, P. et al. Anthropogenic greenhouse gas contribution to flood risk in England and Wales in autumn 2000. *Nature* **470**, 382–385 (2011).

12. Min, S.–K., Zhang, X., Zwiers, F. W. & Hegerl, G. C. Human contribution to more-intense precipitation extremes. *Nature* **470**, 378–381 (2011).

13. Hansen, J., Sato, M. & Ruedy, R. Perception of climate change. *Proc. Natl. Acad. Sci. USA* **109**, 14726-14727 (2012).

14. Field, C.B., *et al*. (eds) *Managing the Risks of Extreme Events and Disasters to Advance Climate Change Adaptation* (Cambridge Univ. Press, 2012).

15. Francis, J. A. & Vavrus, S. J. Evidence linking Arctic amplification to extreme weather in mid-latitudes. *Geophys. Res. Lett.* **39**, L06801 (2012).

16. Liu, J., Curry, J. A., Wang, H., Song, M. & Horton, R. M. Impact of declining Arctic sea ice on winter snowfall. *Proc. Natl. Acad. Sci. USA* **109**, 4074-4079 (2012).

17. Petoukhov, V., Rahmstorf, S., Petri, S. & Schellnhuber, H. J. Quasiresonant amplification of planetary waves and recent Northern Hemisphere weather extremes. *Proc. Natl. Acad. Sci. USA* **110**, 5336-5341 (2013).

18. Screen, J. A. & Simmonds, I. Exploring links between Arctic amplification and mid-latitude weather. *Geophys. Res. Lett.* **40**, 959-964 (2013).

19. Screen, J. A. & Simmonds, I. Caution needed when linking weather extremes to amplified planetary waves. *Proc. Natl. Acad. Sci. USA*, **110**, E2327 (2013).

20. Barnes, E. A. Revisiting the evidence linking Arctic amplification to extreme weather in midlatitudes. *Geophys. Res. Lett.* **40**, 4728-4733 (2013).

21. Leiserowitz, A., Maibach, E., Roser-Renouf, C., Feinberg, G. & Howe, P. *Extreme Weather and Climate Change in the American Mind*. (Yale Univ. & George Mason Univ., 2012).

22. Peings, Y. & Magnusdottir, G. Response of the wintertime Northern Hemisphere atmospheric circulation to current and projected sea ice decline: a numerical study with CAM5. *J. Clim.* doi:10.1175/JCLI-D-13-00272.1 (2013).

23. Screen, J. A. & Simmonds, I. The central role of diminishing sea ice in recent Arctic temperature amplification. *Nature* **464**, 1334-1337 (2010).

24. Serreze, M. C. & Barry, R. G. Processes and impacts of Arctic amplification: A research synthesis. *Global and Planetary Change* **77**, 85-96 (2011).

25. Hoskins, B. J. & Karoly, D. J. The steady linear response of a spherical atmosphere to thermal and orographic forcing. *J. Atmos. Sci.* **38**, 1179-1196 (1981).

26. Teng, H., Branstator, G., Wang, H. Meehl, G. A. & Washington, W. M. Probability of US heat waves affected by a subseasonal planetary wave pattern. *Nature Geoscience* doi:10.1038/ngeo1988 (2013).

27. Jones, P. D., *et al.* Hemispheric and large-scale land surface air temperature variations: an extensive revision and an update to 2010. *J. Geophys. Res.* **117**, D05127 (2012).

28. Adler, R. F., *et al*. The version 2 Global Precipitation Climatology Project (GPCP) monthly precipitation analysis (1979-Present). *J. Hydrometeor.* **4**, 1147-1167 (2003).

29. Dee, D. P., *et al.* The ERA-Interim reanalysis: configuration and performance of the data assimilation system. *Q. J. R. Meteorol. Soc.* **137**, 553–597 (2011).

30. Moser, B. K. & Stevens, G. R. Homogeneity of variance in the two-sample means test. *Amer. Stat.* **46**, 19–21 (1992).

Acknowledgements. CRUTEM4 data were provided by the UK Met Office Hadley Centre (www.metoffice.gov.uk/hadobs); GPCP data by the NOAA Earth System Research Laboratory (www.esrl.noaa.gov/psd/data); and ERA-Interim data by the ECMWF (apps.ecmwf.int/datasets). This research was funded by UK Natural Environment Research Council grant NE/J019585/1 awarded to J. A. S.

Author Contributions. J. A. S. designed and performed research, analysed data and wrote the paper. I. S. discussed the results and commented on the manuscript.

Tables

Table 1: Differences in planetary-wave amplitude anomalies between months of extreme weather and climatology.

	Hot		Cold		Wet		Dry	
	t	f	t	f	t	f	t	f
wNAm	***2.31***	***1.22***	-0.05	1.13	0.71	1.07	1.05	1.05
cNAm	1.11	***1.19***	1.48	***1.21***	***-1.80***	-1.09	***2.52***	***1.25***
eNAm	-1.18	-1.02	***3.54***	***1.37***	1.08	***1.18***	0.25	1.03
Euro	0.78	1.00	1.15	1.01	0.08	1.02	***2.54***	1.10
wAsia	-0.45	-1.12	0.70	-1.03	***2.45***	1.03	-0.86	-1.01
cAsia	***3.11***	1.02	0.28	1.11	0.25	-1.01	***2.94***	1.11
eAsia	-1.24	-1.12	0.12	1.14	-0.04	***1.21***	-0.05	-1.07

The t and f statistics corresponding to, respectively, differences in mean planetary-wave amplitude and differences in amplitude variance between composites of months with extreme weather and climatology. Statistics are provided separately for four types of weather extreme (hot, cold, wet and dry) and for eight geographical regions. Differences in mean amplitude or variance that are significant at the 90% confidence level are shown in bold italic type. Regions and their abbreviations are shown in Fig. 3.

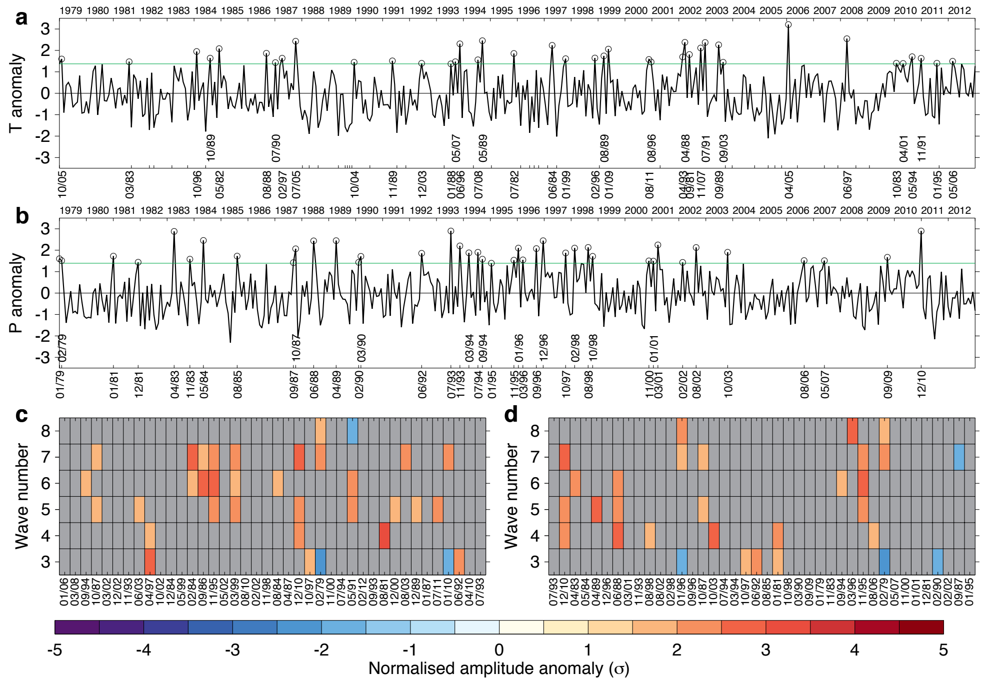

Figure 1: Planetary-wave amplitude anomalies during months of extreme weather. Normalised monthly time-series of mid-latitude- (35-60°N) mean land-based absolute temperature anomalies (**a**) and absolute precipitation anomalies (**b**), 1979-2012. In **a** and **b**, the 40 months with largest values are identified by circles and labelled on the lower x-axis, and the green line shows the threshold value for extremes. Normalised wave amplitude anomalies, for wave numbers 3-8, during 40 months of mid-latitude- mean temperature extremes (**c**) and precipitation extremes (**d**). In **c** and **d**, the months are labelled on the abscissa in order of decreasing extremity from left to right. Grey shading masks anomalies that are not statistically significant at the 90% confidence level; specifically, anomalies with magnitude smaller than 1.64σ, the critical value of a Gaussian (normal) distribution for a two-tailed probability p = 0.1. Red shading indicates wave numbers that are significantly amplified compared to average and blue shading indicates wave numbers that are significantly attenuated compared to average.

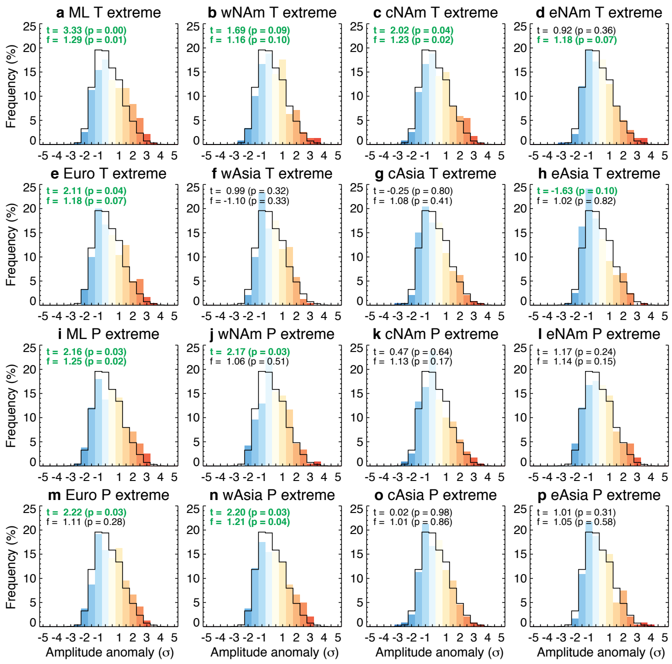

Figure 2: Frequency distributions of planetary-wave amplitude anomalies during months of extreme weather. Probability density functions (PDFs) for normalised wave amplitude anomalies (wave numbers 3-8) during 40 months of extreme temperature over eight geographical regions: ML (**a**), wNAm (**b**), cNAm (**c**), eNAm (**d**), Euro (**e**), wAsia (**f**), cAsia (**g**) and eAsia (**h**); and during 40 months of extreme precipitation over the same 8 regions (**i-p**), respectively. The coloured bars show the relative frequency (expressed as a percentage of the total number of anomalies) of amplitude anomalies in bins of 0.5σ. The black lines show the climatological frequencies. The t and f statistics and their associated p values are provided, with bold green text highlighting values that are statistically significant at the 90% confidence level. The regions and their abbreviations are shown in Fig. 3.

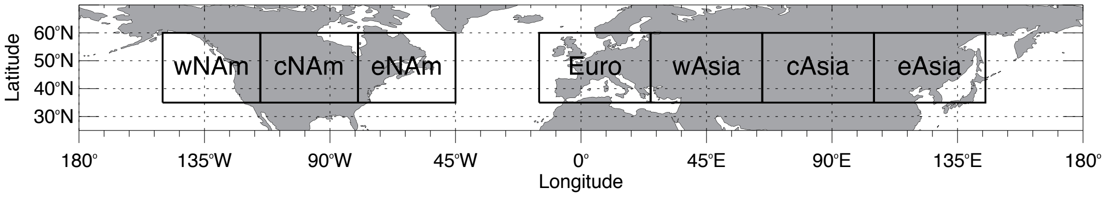

Figure 3: The geographical regions used in this study. Black boxes show the regions and are labelled with their abbreviations.

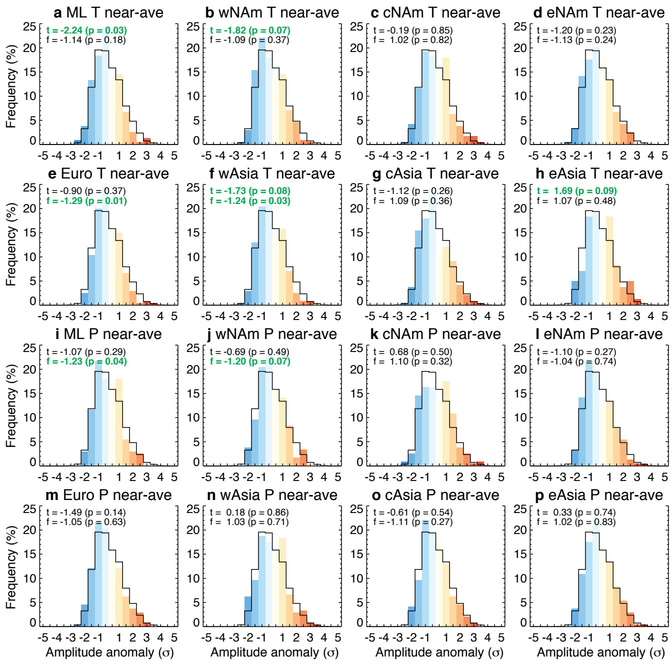

Figure 4: Frequency distributions of planetary-wave amplitude anomalies during months of near-average weather. As Fig. 2, but for months of near-average temperature (**a-h**) and precipitation (**i-p**).